Measurement of High Temperature Elastic Moduli of Infrared Transparent Materials

August 1998

D.W. Blodgett and K.C. Baldwin
The Johns Hopkins University Applied Physics Laboratory
Laurel, MD 20723

J.B. Spicer
The Johns Hopkins University
Materials Science and Engineering Department
Baltimore, MD 21218

ABSTRACT

Insight into a material's high temperature mechanical and microstructural properties can be gained from knowledge of its elastic moduli. For a single-crystal material, the elastic modulus, C_{ijkl}, provides information on the strain (ε_{kl}) - stress (σ_{ij}) relationship given by $\sigma_{ij} = C_{ijkl} \bullet \varepsilon_{kl}$. This relationship shows that, for a given strain, a large elastic modulus will induce a large stress in the material. In regards to mechanical properties, the crystallographic axis with the largest elastic modulus is the most likely for failure to occur. Before any IR transparent material can be considered for application in a high stress environment, such as IR dome applications, the elastic moduli must be known.

Laser-based ultrasonics provides a non-contact, non-destructive means of measuring the elastic moduli of IR transparent materials in an elevated temperature environment. In this paper, the application of laser ultrasonics to IR materials characterization is reviewed. Specific calculations for determining the elastic moduli for isotropic and trigonal crystal symmetries, as exhibited by single-crystal sapphire, are presented. Measurements of the elastic moduli as a function of temperature for borosilicate glass and fused silica, elastically isotropic materials, are presented. In addition, a room-temperature ultrasonic measurement of germanium (Ge), an elastically anisotropic material, is shown.

1.0 INTRODUCTION

The high temperature behavior of infrared (IR) transparent materials is not well understood owing to the wide-ranging property variations. For high stress environments, such as those encountered by IR missile domes, the IR material's mechanical properties must be known. A critical figure of merit for determining the suitability of candidate IR dome materials is the thermal shock resistance. A material's thermal shock resistance, R, is proportional to

$$R \propto \frac{S(1-\nu)}{E} \qquad \textbf{(1)}$$

where S is the mechanical strength, ν is the Poisson's ratio, and E is the elastic modulus. Both the mechanical strength and elastic moduli are known to be highly temperature dependent. Therefore, both must be known for a complete understanding of the material's high-temperature behavior. The most common means of measuring the mechanical strength of a material is through fracture tests, which provide information on the applied load necessary to induce fracture in the material [1]. For brittle materials, such as ceramics, these tests are heavily dependent on the surface quality of the specimen. Any surface cracks

or abrasions can lead to premature failure of the sample, indicating lower fracture toughness. For this reason, a statistically large number of samples are typically tested to establish a mean fracture strength [2]. The elastic modulus, E (or C_{ijkl} for a single-crystal material), is a measure of the linear relation between the applied strain and the resulting stress in a material. Means for measuring the elastic moduli of a material include both static (i.e. flexure) and dynamic (i.e. vibrational or ultrasonic) [2]. Static flexure tests suffer from nonuniform stress distribution and a stress distribution that changes with increasing strain if some plastic deformation occurs. These considerations limit the accuracy of the elastic moduli measurement to a few percent. Dynamic methods, such as ultrasonics, can achieve better than an order of magnitude greater accuracy than static methods [2].

In ultrasonics, the velocities of the longitudinal and shear waves are measured, which allow the elastic moduli to be determined. In anisotropic materials, up to three bulk acoustic waves can be supported, each with its own characteristic velocity. Conventional ultrasonics uses a contact transducer to both generate and detect the ultrasonic waves [3]. Unfortunately, the lack of high-temperature transducer couplant limits the maximum temperature at which contact ultrasonic measurements can be made. In an effort to extend the temperature range over which contact ultrasonic measurements can be made, Papadakis *et al.* [4] developed a momentary contact technique. In this technique, a long, cool buffer rod is placed in momentary contact (~100 ms) with the sample. A contact transducer mounted on the end of the rod is then used to both transmit the ultrasonic signal and receive the ultrasonic echo. This technique has successfully measured the elastic properties of materials up to 1200 °C.

Laser based ultrasonics replaces the contact transducer, used for generation, with a short laser pulse. When the laser pulse interacts with the sample, both reflection and absorption occur. As a result of absorption, temperature gradients are established within the solid, which produce a rapidly changing strain field. This strain field, in turn, radiates energy as elastic (ultrasonic) waves. At low pulse energies, this is an entirely thermoelastic process (i.e. non-destructive).

Optical detection of the ultrasonic arrivals provides a complementary non-contact technique for high-temperature ultrasonic measurements. Two common methods are optical beam deflection and interferometric detection [5]. Optical beam deflection focuses a laser onto the surface of the specimen and knife-edges the reflected beam onto a detector. When the ultrasonic wave arrives, it causes a small surface displacement, deflecting the focused beam and varying the optical power reaching the detector. In interferometric detection, the surface displacement from the ultrasonic arrival varies the optical path length of one arm of the interferometer. This path length variation causes a corresponding change in the phase of the optical signal. The interferometer converts this phase change to intensity variations, which can then be measured directly (see Figure 1).

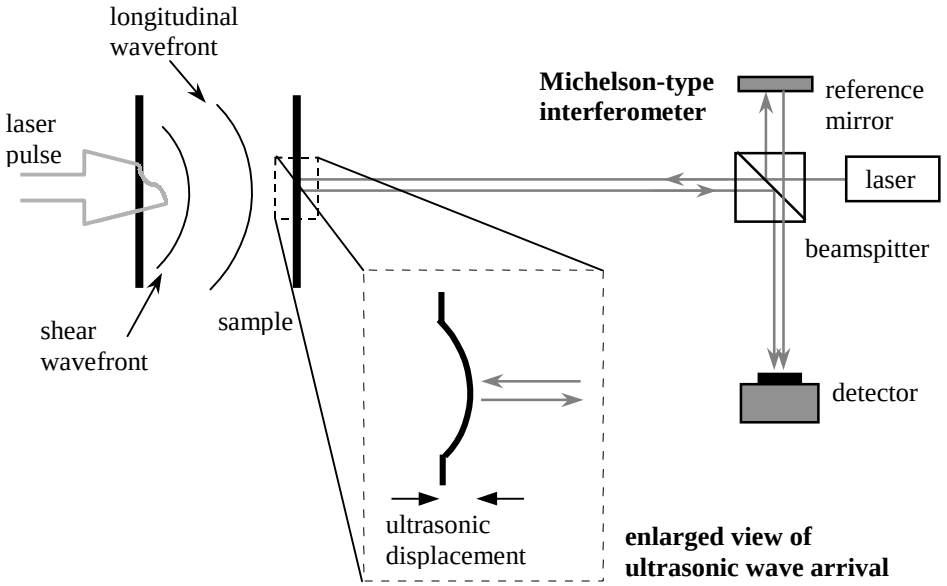

Figure 1. Ultrasonic measurement using a pulsed-laser for ultrasonic wave generation and a Michelson-type interferometer for ultrasonic wave detection.

2.0 THEORY

In general, three different bulk elastic waves may propagate in any given direction in an anisotropic material. In general, these waves are not pure modes, that is, they contain displacement components both parallel and perpendicular to the wavefront normal. The governing equation for stress wave propagation in an elastic solid is given by [6,7]

$$\sigma_{ij,j} + X_i = \rho \ddot{u}_i \tag{2}$$

where σ_{ij} is the stress tensor, X_i is the body force, ρ is the material density, and u_i is the displacement vector. For an elastic anisotropic solid, the stress is linearly related to the strain (ε_{kl}) through the elastic modulus (C_{ijkl}).

$$\sigma_{ij} = C_{ijkl}\varepsilon_{kl} \tag{3}$$

The symmetric strain for a material can be defined in terms of displacements as

$$\varepsilon_{kl} = \frac{1}{2}\left(u_{k,l} + u_{l,k}\right) \tag{4}$$

Substituting Eq. 4 into Eq. 2 yields (due to the symmetric nature of the elastic modulus)

$$\sigma_{ij} = \frac{1}{2}C_{ijkl}\left(u_{k,l} + u_{l,k}\right) \tag{5}$$

Now, due to the symmetric nature of the elastic modulus (with $C_{ijkl} = C_{klij} = C_{jikl} =$, …), Eq. 4 can be reduced to

$$\sigma_{ij} = C_{ijkl}u_{k,l} \tag{6}$$

The wave equation can now be written in terms of the displacement vectors. Under the assumption of no body forces, $X_i = 0$:

$$C_{ijkl}\, u_{k,lj} - \rho \ddot{u}_i = 0 \tag{7}$$

For bulk wave propagation, the form of the displacement vector is given by

$$u_k = A_0\alpha_k e^{i(\omega t - k_m x)} \tag{8}$$

where A_0 is the displacement amplitude, α_k is the direction cosine of the displacement vector, ω is the angular frequency, and k_m is the wave vector. Rewriting the wave vector in terms of the direction cosines, l_m, of the normal to the wave front yields

$$\begin{aligned} k_m &= \left(\frac{2\pi}{\lambda}\right)l_m \\ &= k l_m \end{aligned} \tag{9}$$

Substituting Eq. 8 into Eq. 7 yields

$$C_{ijkl}k^2 l_l l_j u_k - \rho\omega^2 u_i = 0 \tag{10}$$

which can be rewritten, when $u_i = \delta_{ik}u_k$ and δ_{ik} = kronecker delta function, as

$$\left(C_{ijk}l_l l_j - \rho v^2\delta_{ik}\right)u_k = 0 \tag{11}$$

Since the components of the displacement vector in Eq. 11 are not necessarily equal to zero, the expression that proceeds it must be identically equal to zero such that

$$\left|C_{ijk}l_l l_j - \rho v^2\delta_{ik}\right| = 0 \tag{12}$$

Rewriting Eq. 12 in terms of its components:

$$\begin{vmatrix} C_{1jk}l_k l_j - \rho v^2 & C_{1jk2}l_k l_j & C_{1jk3}l_k l_j \\ C_{2jk1}l_k l_j & C_{2jk2}l_k l_j - \rho v^2 & C_{2jk3}l_k l_j \\ C_{3jk1}l_k l_j & C_{3jk2}l_k l_j & C_{3jk3}l_k l_j - \rho v^2 \end{vmatrix} = 0 \tag{13}$$

Recalling that the elastic modulus relates the symmetric stress to the symmetric strain, the maximum number of matrix elements is reduced to 21. Further reduction occurs when a specific crystallographic system is chosen. For an isotropic material, such as a glass or any polycrystalline ceramic, the number of independent elastic moduli reduces to two [8]. For wave propagation along the +x1 direction (see Figure 2), the direction cosines for the specimen axis (SA) reduce to:

$l_1 = \sin\theta\cos\phi = 1;$
$l_2 = \sin\theta\sin\phi = 0;$
$l_3 = \cos\theta.$

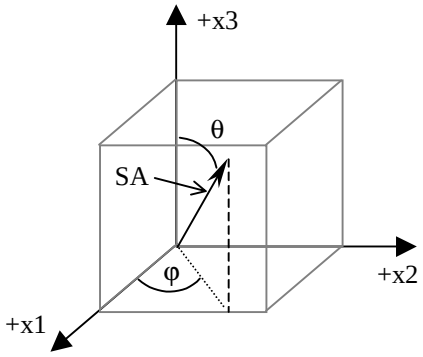

Figure 2. System of wave propagation.

Therefore, for an isotropic material, Eq. 13 reduces to (using reduced notation [8] for the elastic modulus)

$$\begin{vmatrix} C_{11} - \rho v^2 & 0 & 0 \\ 0 & C_{44} - \rho v^2 & 0 \\ 0 & 0 & C_{44} - \rho v^2 \end{vmatrix} = 0 \qquad \textbf{(14)}$$

Solving for Eq. 14 yields two propagation velocities, one longitudinal and one shear, given by

$$v_{long} = \sqrt{\frac{C_{11}}{\rho}} = \sqrt{\frac{\lambda + 2\mu}{\rho}} \quad \text{and} \quad v_{shear} = \sqrt{\frac{\mu}{\rho}} \qquad \textbf{(15)}$$

where λ is the Lamé constant and μ is the shear modulus. Therefore, by measuring the arrival times of the longitudinal and shear waves and having knowledge of the sample's thickness, the two elastic constants for an isotropic material to be determined. This shows that only a single sample is required for complete characterization of the elastic moduli of an isotropic material.

The lower symmetry of crystalline materials increases the number of moduli that must be determined. One of the most common crystalline materials for high stress environments is single crystal sapphire. Single-crystal sapphire displays trigonal symmetry, increasing the number of independent elastic moduli components to six. This greatly increases the complexity of the determinant (Eq. 12) which must be solved. Following the presentation by Wachtman *et al*. [9], the determinant can be written in the form

$$\begin{vmatrix} A - \rho v^2 & H & G \\ H & B - \rho v^2 & F \\ G & F & C - \rho v^2 \end{vmatrix} = 0 \qquad \textbf{(16)}$$

where $A = C_{11}l_1^2 + C_{66}l_2^2 + C_{44}l_3^2 + 2C_{14}l_2l_3$
$B = C_{66}l_1^2 + C_{11}l_2^2 + C_{44}l_3^2 - 2C_{14}l_2l_3$
$C = C_{44}(l_1^2 + l_2^2) + C_{33}l_3^2$
$F = C_{14}(l_1^2 - l_2^2) + (C_{13} + C_{44})l_2l_3$
$G = 2C_{14}l_1l_2 + (C_{13} + C_{44})l_1l_3$
$H = (C_{12} + C_{66})l_1l_2 + 2C_{14}l_1l_3$
$C_{66} = \frac{1}{2}(C_{11} - C_{12})$

Following a similar procedure to that outlined above for isotropic materials, propagating a stress wave along the c-axis (i.e. along +x3 with $\theta = 0°$ and $\varphi = 90°$) yields two characteristic wave velocities given by

$$v_1 = \sqrt{\frac{C_{33}}{\rho}} \tag{17}$$

$$v_2 = \sqrt{\frac{C_{44}}{\rho}} \tag{18}$$

This allows for the determination of C_{33} and C_{44}. Propagation along the m-xis (i.e. along +x2 with $\theta = 90°$ and $\varphi = 90°$) yields three ultrasonic wave arrivals. These waves provide information on C_{11}, C_{12} and C_{14}.

$$v_3 = \sqrt{\frac{C_{11} - C_{12}}{\rho}} \tag{19}$$

$$v_4, v_5 = \left[\frac{1}{2\rho}\left\{(C_{11} + C_{44}) \pm \sqrt{C_{11}^2 + C_{44}^2 + 4C_{14}^2 - 2C_{11}C_{44}}\right\}\right]^{1/2} \tag{20}$$

To completely determine these elastic moduli, ultrasonic waves can be propagated along the a-axis (i.e. along +x1 with $\theta = 90°$ and $\varphi = 0°$). As with propagation along the m-axis, three ultrasonic wave arrivals are detected with characteristic velocities of

$$v_6 = \sqrt{\frac{C_{11}}{\rho}} \tag{21}$$

$$v_7, v_8 = \left[\frac{1}{2\rho}\left\{\frac{1}{2}(C_{11} - C_{12}) + C_{44} \pm \sqrt{\frac{1}{4}(C_{11} - C_{12})^2 - C_{44}(C_{11} - C_{12}) + C_{44}^2 + 4C_{14}^2}\right\}\right]^{1/2} \tag{22}$$

These velocity measurements allow for five of the six elastic moduli for single-crystal sapphire to be measured. The remaining elastic moduli, C_{13}, can be measured by propagating the ultrasonic waves off of one of the crystallographic axis (i.e. at $\theta = 45°$ and $\varphi = 0°$). Thus, by choosing three appropriately oriented samples, all of the elastic constants can be determined.

3.0 EXPERIMENT

The materials chosen for this work included fused silica, borofloat™ borosilicate, and single-crystal sapphire. While all of these are transparent in the IR, they possess very different elastic properties. The fused silica and borofloat™ borosilicate are both amorphous materials and, therefore, elastically isotropic in nature. In contrast, single-crystal sapphire displays trigonal symmetry. The approximate IR transmission band and other physical properties for each of these materials are listed in Table 2.

Table 1. IR transmission band for selected materials [10]

Material	**Transmission Band [μm]**		**Density**	**Melt. Temp.**	**Therm. Cond.**	**Therm. Expansion**
	Begin	**End**	**[g/cm^3]**	**[°C]**	**[W/m°C]**	**[1/°C]**
fused silica	0.2	4.5	2.202	990‡	1.6*	0.75x10^{-6} **
borofloat™ borosilicate	0.3	3	2.2	450	1.12	3.25x10^{-6}
single-crystal sapphire (0°)	0.15	6	3.98	2027	35.1†	5.6x10^{-6} †
single-crystal sapphire (90°)	0.15	6	3.98	2027	33.0†	5.0x10^{-6} †
germanium (optical grade)	1.2	15	5.35	937	165.8	2.4x10^{-6} †

* at 373 K, ** at 423 K, ‡ glass transition temperature, † at 300 K

The experimental set-up used to measure the elastic constants, as a function of temperature, is shown in Figure 3. Samples were placed in the center of the high-temperature furnace, which has optical

access ports on two sides. A pulsed Nd:YAG laser (1.064 μm) with a 20 ns pulse duration (FWHM) was used to generate the ultrasound on the backside of the sample.

Due to the IR transparent nature of the materials, each was coated with a 50 nm TiW film to aid in the generation and detection of ultrasound. It is important that the laser pulse be absorbed at the surface for the generation of the high-frequency ultrasound needed for precise measurement of wave arrival times. The absorption coefficient for tungsten at 1.064 μm is given by

$$\alpha = \frac{4\pi\kappa}{\lambda} = \frac{4\pi(4)}{1.064\,\mu m} = 47.2\,\mu m^{-1} \quad \textbf{(23)}$$

where κ is the extinction coefficient of tungsten at 1.1 μm. This absorption coefficient corresponds to an absorption depth of about 21 nm. It should be noted that these films are thin enough that they do not interfere with the ultrasonic wave propagation as their thickness is far less than that of a typical generated ultrasonic wavelength. For fused silica, for example, ultrasonic velocities are on the order of 5 mm/μs, corresponding to a minimum wavelength of 0.17 mm at 30 MHz. In the future, a pulsed CO2 laser, which is highly absorbed by each of the materials, will be used for ultrasonic generation. This will alleviate the need for the TiW coating.

A stabilized Michelson-type interferometer [3] is used to detect the ultrasonic wave arrival. This type of interferometer is sensitive to displacements normal to the surface and is inherently uniform in its frequency response characteristics. The output signal of the interferometer was captured using a digital oscilloscope, which was triggered by the arrival of light scattered from the generation laser pulse. The bandwidth for these measurements was limited to less than 30 MHz.

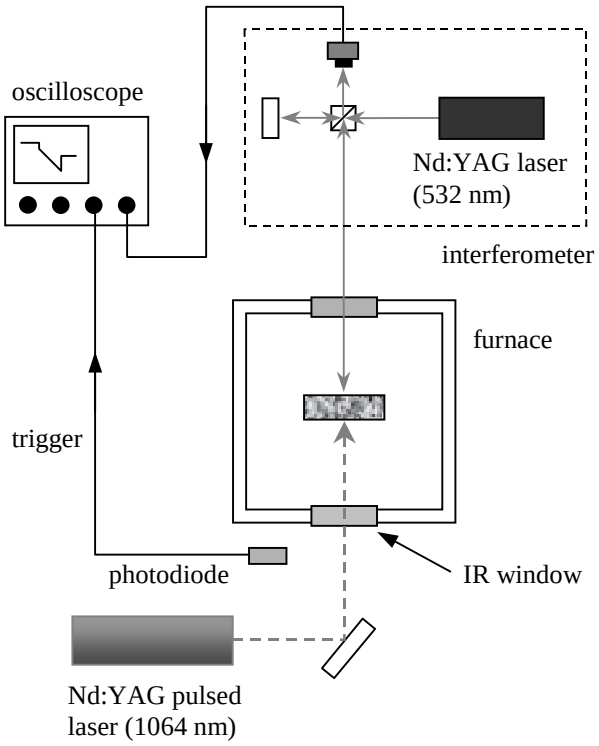

Figure 3. Experimental set-up for high-temperature ultrasonic measurements.

4.0 RESULTS

Results for epicentral laser ultrasonic waveforms in borofloat™ borosilicate, at three different temperatures, are shown in Figure 4. The change in arrival times for the longitudinal and shear waves is

attributed to variations in the elastic moduli of the material as a function of temperature. As shown in Eq. 15, the Lamé constant and shear modulus can be calculated from knowledge of the two wave velocities. A plot of the Lamé constant and shear modulus, as a function of temperature, is given in Figure 5. At 325 °C, there is a sharp drop in the moduli, indicating a possible microstructural change in the material. This may be attributed to a rearrangement of the boron ions in the glass. These modulus values are typical for borosilicate glasses [12].

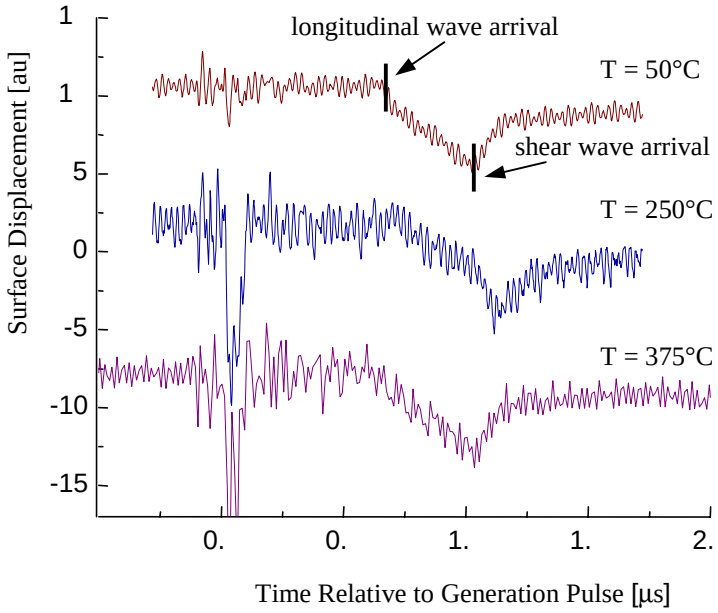

Figure 4. Ultrasonic waveforms for borofloat™ borosilicate as a function of temperature.

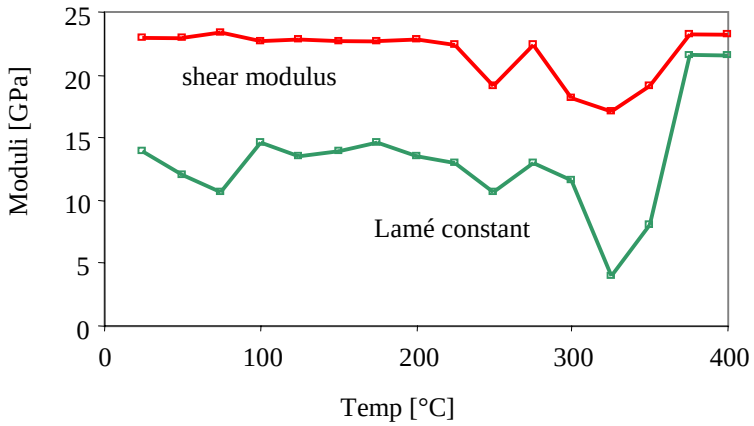

Figure 5. Variations in elastic moduli of borofloat™ borosilicate as a function of temperature.

Similar measurements were made for fused silica, which has a much higher operating temperature. Figure 6 shows a plot of the elastic moduli as a function of temperature. Unlike the moduli for the borosilicate glass, these measurements show a constant increase in the elastic moduli. To avoid oxidation of the Ti/W film at these higher temperatures, a reducing atmosphere (5% Hydrogen/95% Argon mixture) was flowed through the furnace.

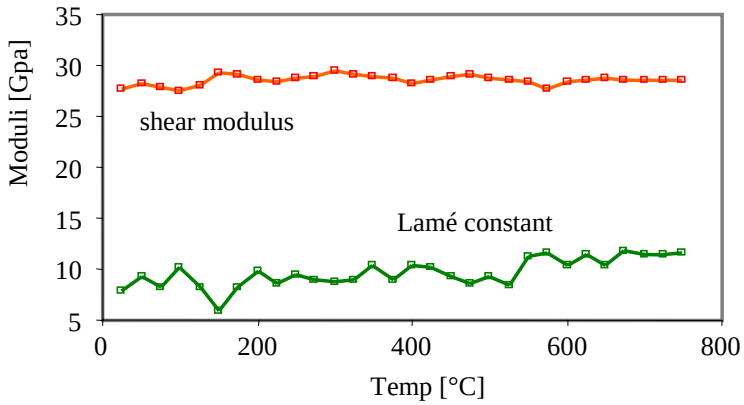

Figure 6. Variations in elastic moduli of fused silica as a function of temperature.

Each of the above samples is transmissive over the visible to the mid-IR spectrum. However, Ge's transparency begins at about 1.2 μm and extends to the far-IR. Due to its high-absorption at 1 μm, the TiW film was not needed for ultrasound generation. The addition of the TiW film for the previous samples, although allowing for ultrasound generation using the Nd:YAG laser, limited the amount of pulse energy that could be used before ablating the film. This ablation limit contributed to the poor SNR of the previously shown waveforms. A room temperature ultrasonic waveform for Ge is given in Figure 7. The improved SNR is readily apparent and this waveform shows a distinct longitudinal arrival and two shear arrivals. Germanium has a cubic crystal class with a diamond crystal structure. The diamond crystal structure is anisotropic with three elastic moduli. It is this anisotropy that leads to the two shear wave arrivals.

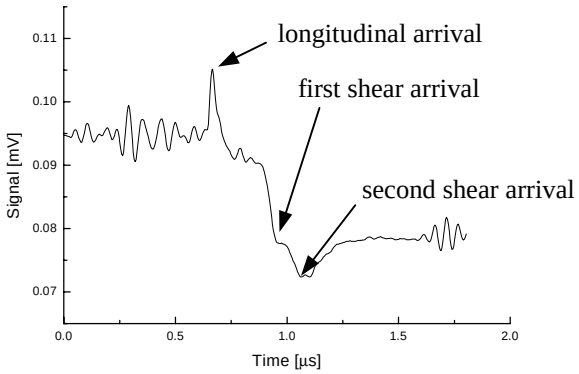

Figure 7. Room temperature ultrasonic waveform for Ge.

5.0 CONCLUSIONS

The application of laser ultrasonics to the measurement of the high temperature elastic moduli of IR transparent materials has been presented. Knowledge of a material's elastic moduli and mechanical strength allow for its thermal shock resistance to be determined. The thermal shock resistance is an important parameter to determine a material's suitability for IR dome applications. Calculations for isotropic and trigonal materials have been presented. These calculations show that at most three samples, with specified crystallographic orientations, are required for the determination of all six elastic moduli in sapphire. Measurements of the elastic moduli, as a function of temperature, of two IR transparent materials, borofloat™ borosilicate and fused silica, are given. Measurements in the borosilicate glass show a sudden drop in the elastic moduli at about 225 °C. This is believed due to motion of the boron atoms in the glass structure. In contrast, the elastic moduli of the fused silica are shown to increase slightly as the

temperature is increased. Both of these measurements suffered from relatively poor SNR due to the ablation threshold of the TiW film. Using a pulsed laser that is highly absorbed by the samples would alleviate the need for the film and allow for more pulse energy to be used in ultrasonic generation. A room temperature ultrasonic measurement for Ge was also presented. This waveform has a much improved SNR due to its better absorption characteristics at the Nd:YAG pulse wavelength. In addition, the measurement clearly shows two shear wave arrivals due to the diamond crystal structure of the sample. Work is currently underway to make high-temperature elastic moduli measurements on single-crystal sapphire samples.

6.0 ACKNOWLEDGEMENTS

This work was supported through the IR&D program at the Johns Hopkins University Applied Physics Laboratory (JHU/APL). The authors are grateful to Phil McNally of the Technical Services Department at JHU/APL for coating the samples for these experiments.

7.0 REFERENCES

1) T.H. Courtney, Mechanical Behavior of Materials, McGraw-Hill (1990).
2) J.B. Wachtmann, Mechanical Properties of Ceramics, John Wiley & Sons (1996).
3) C.B. Scruby and L.E. Drain, Laser Ultrasonics: Techniques and Applications, Adam-Hilger (1990).
4) E.P. Papadakis, L.C. Lynnworth, K.A. Fowler, and E.H. Carnevale, "Ultrasonic Attenuation and Velocity in Hot Specimens by the Momentary Contact Method with Pressure Coupling, and Some Results on Steel to 1200°C", J. Acoust. Soc. Amer., 52(3) pp850-857 (1972).
5) J.W. Wagner, Physical Acoustics XIX: Optical Detection of Ultrasound, Academic Press, pp201-266 (1990).
6) R.E. Green, Treatise on Materials Science and Technology, Vol. 3: Ultrasonic Investigation of Mechanical Properties, Academic Press (1973).
7) K.F. Graff, Wave Motion in Elastic Solids, Dover Publications (1991).
8) J.F. Nye, Physical Properties of Crystals, Oxford Science Publications (1985).
9) J.B. Wachtman, W.E. Tefft, D.G. Lam, and R.P. Stinchfield, "Elastic Constants of Synthetic Crystal Corundum at Room Temperature", J. Res. NBS-A, Vol. 64A(3), pp213-227.
10) P. Klocek, Handbook of Infrared Optical Materials, Dekker Publications (1991).
11) D.E. Gray, American Institute of Physics Handbook, McGraw-Hill (1972).
12) N.P. Bansal and R.H. Doremus, Handbook of Glass Properties, Academic Press (1986).